The Cell Wall of the Pathogenic Bacterium *Rhodococcus equi* Contains Two Channel-Forming Proteins with Different Properties

Franziska G. Rieβ,[1] Marion Elflein,[1] Michael Benk,[1] Bettina Schiffler,[1] Roland Benz,[1]* Natalie Garton,[2] and Iain Sutcliffe[2]

Lehrstuhl für Biotechnologie, Biozentrum der Universität Würzburg, Am Hubland, D-97074 Würzburg, Germany,[1] and University of Sunderland, Institute of Pharmacy, Fleming Building, Sunderland SR2 3SD, England[2]

We have identified in organic solvent extracts of whole cells of the gram-positive pathogen *Rhodococcus equi* two channel-forming proteins with different and complementary properties. The isolated proteins were able to increase the specific conductance of artificial lipid bilayer membranes made from phosphatidylcholine-phosphatidylserine mixtures by the formation of channels able to be permeated by ions. The channel-forming protein $PorA_{Req}$ (*R. equi* pore A) is characterized by the formation of cation-selective channels, which are voltage gated. $PorA_{Req}$ has a single-channel conductance of 4 nS in 1 M KCl and shows high permeability for positively charged solutes because of the presence of negative point charges. According to the results of sodium dodecyl sulfate-polyacrylamide gel electrophoresis (SDS-PAGE), the protein has an apparent molecular mass of about 67 kDa. The analysis (using the effect of negative charges on channel conductance) of the concentration dependence of the single-channel conductance suggested that the diameter of the cell wall channel is about 2.0 nm. The second channel (formed by $PorB_{Req}$ [*R. equi* pore B]) shows a preferred movement of anions through the channel and is not voltage gated. This channel shows a single-channel conductance of 300 pS in 1 M KCl and is characterized by the presence of positive point charges in or near the channel mouth. Based on SDS-PAGE, the apparent molecular mass of the channel-forming protein is about 11 kDa. Channel-forming properties of the investigated cell wall porins were compared with those of others isolated from mycolic acid-containing actinomycetes. We present here the first report of a fully characterized anion-selective cell wall channel from a member of the order *Actinomycetales*.

Rhodococcus equi (formerly *Corynebacterium equi*) is recognized as a significant cause of disease in foals between the ages of 1 and 6 months and is responsible for ca. 3% of global foal mortality (13, 33). This organism was first reported as a cause of human disease in 1967 (14), since which time it has emerged as an opportunistic pathogen, notably (but not exclusively) of patients with compromised immunity (25, 27, 33, 52). Moreover, it is likely that the incidence of human infection by *R. equi* has been underestimated through either misdiagnosis or unwarranted dismissal of the organism as a contaminant diphtheroid (52).

In both foals and humans, *R. equi* disease is typically characterized by bronchopneumonia, although extrapulmonary manifestations are also found (13, 33, 52). *R. equi* is an intracellular pathogen of alveolar macrophages, and the bacterium is known to enter macrophages via complement receptors following deposition of complement component C3 (25). Once within the macrophage, the bacteria resist the host's killing mechanisms and multiply. However, there is currently little information concerning the specific bacterial factors which facilitate entry into or subsequent survival within macrophages. Persistence within macrophages most likely contributes to the in vivo resistance of *R. equi* to many classes of antibiotics (13). A combination of rifampin and erythromycin remains the treatment of choice for foals, but no optimal drug regimen has been established for human infections and relapse is a significant problem (52). Moreover, rifampin-resistant phenotypes of *R. equi* have been identified (1, 12, 49), and the use of erythromycin in foals may have side effects (13, 46). There thus remains a need to identify physiological features of *R. equi* that contribute to the ability of this organism to thrive within macrophages and which might provide targets for the implementation of novel therapeutic strategies.

R. equi is a member of a unique bacterial taxon, the mycolata, within the gram-positive actinomycetes (9). Members of this taxon are distinguished by the presence within their cell envelopes of large 3-hydroxy 2-alkyl branched fatty acids, the mycolic acids (MAs). A large proportion of the MAs are covalently linked to the arabinogalactan cell wall polysaccharide, and in contrast to the typical gram-positive cell envelope, an outer lipid permeability barrier is predicted to be formed by the association of these bound MAs with other cell envelope lipids, such as trehalose mycolates (8, 10, 15, 24, 32, 35, 47, 48). The presence of this asymmetric outer lipid permeability barrier predicates that the cell envelopes of the mycolata must contain permeability pathways accessible to hydrophilic solutes. Consistent with this, cation-selective channel-forming proteins have been identified in the cell walls of *C. diphtheriae* (35), *C. glutamicum* (20, 23, 29), *Mycobacterium bovis* (21), *M. chelonae* (50), *M. phlei* (38), *M. smegmatis* (26, 30, 51), *M. tuberculosis* (16, 45), *Nocardia asteroides* (39), *N. (Rhodococcus) corynebacteroides* (37), *N. farcinica* (40), and *R. erythropolis* (22). The selectivity of these channels for cations suggests that the cell walls of these MA-containing actinomycetes also contain complementary channels of distinct specificities. Consis-

* Corresponding author. Mailing address: Lehrstuhl für Biotechnologie, Biozentrum der Universität Würzburg, Am Hubland, D-97074 Würzburg, Germany. Phone: 49 (0) 931-888-4501. Fax: 49 (0) 931-888-4509. E-mail: roland.benz@mail.uni-wuerzburg.de.

tent with this, an anion-selective channel has also been identified in *M. bovis* (21).

To extend these studies on the channel-forming proteins of the mycolata and to further strengthen our understanding of cell envelope permeability in an important pathogen, we have investigated the presence of channel-forming activities in the cell wall of *R. equi*. The results suggest that the cell wall of this pathogen contains at least two types of channels: a high-conductance cation-selective channel and a low-conductance anion-selective channel.

MATERIALS AND METHODS

Growth and maintenance of microorganisms. The type strain of *R. equi* ATCC 6939 was supplied by John Prescott (University of Guelph, Ontario, Canada). Stock cultures were maintained on slopes of brain heart infusion (BHI) agar (Oxoid; Unipath Ltd., Basingstoke, United Kingdom) at 4°C. Cultures were maintained by routine subculture onto BHI agar and growth at 37°C for 18 h. Broth cultures were grown in BHI broth incubated at 37°C with shaking (200 rpm) for 18 h. The grown cultures were then harvested by centrifugation (3,500 × g, 4°C, 10 min), washed twice in phosphate-buffered saline, and lyophilized.

SDS-PAGE. Analytical and preparative sodium dodecyl sulfate-polyacrylamide gel electrophoresis (SDS-PAGE) on Tricine-containing gels was performed according to a method previously described (42). The gels were stained with Coomassie brilliant blue or colloidal Coomassie blue (11).

Isolation and purification of the channel-forming proteins from the cell wall. The lyophilized cells were inspected for channel-forming activity by treatment with organic solvents, as this method has successfully been used previously for the identification and purification of the cell wall porins of *C. glutamicum* (20) and *R. erythropolis* (22). Lyophilized cells (0.2 g) were extracted with 8 ml of a 1:2 mixture of $CHCl_3$:CH_3OH for 24 h at 50°C by stirring in a closed container to avoid the loss of $CHCl_3$. The cell-$CHCl_3$:CH_3OH mixture was centrifuged at 10,000 rpm at 4°C for 20 min in a Beckmann J2-21 M/E centrifuge (rotor JA20). The pellet was discarded, and the supernatant extract was mixed with ice-cold diethylether in a ratio of 1 part supernatant to 9 parts diethylether and kept overnight at −20°C. The precipitated protein was dissolved in a solution containing 1% Genapol and 10 mM Tris-HCl (pH 8.0) followed by a second precipitation step with ice-cold diethylether. This second precipitation step reduced the lipid content of the samples. The final pellet contained the channel-forming protein PorB$_{Req}$ (*R. equi* pore B), as determined by black-lipid bilayer experiments (see below). Treatment of the dissolved protein fraction with 2.5 volumes of ice-cold ethanol for 24 h at −20°C followed by centrifugation yielded a pellet that was dissolved in a solution containing 1% Genapol and 10 mM Tris-HCl (pH 8.0) and was incubated for 2 days at room temperature. Inspection of this preparation for channel-forming activity led to the discovery of the channel-forming protein PorA$_{Req}$ (*R. equi* pore A).

Lipid bilayer experiments. The method used for the experiments investigating reconstitution by the black lipid bilayer membranes has been described previously (5). The membranes were formed from a 1% (wt/vol) solution of a mixture of diphytanoyl phosphatidylcholine (PC) and phosphatidylserine (PS) (both lipids were obtained from Avanti Polar Lipids, Alabaster, Ala.) in a molar ratio of 4:1 in *n*-decane. Membranes were also formed from PC-MA (Sigma) or PC-PS-MA mixtures to study the effect of MAs on channel formation. The membrane current was measured with a pair of calomel electrodes switched in series with a voltage source and an electrometer (Keithley 617). For single-channel recordings, the electrometer was replaced by a highly sensitive current amplifier (Keithley 427). Using a high-impedance electrometer (Keithley 617) as described earlier (6), zero-current membrane potentials were measured by establishing a salt gradient across membranes containing 100 to 1,000 channels.

Estimation of the channel diameter using the Renkin correction factor. The calculation of the channel size is possible from single-channel conductance data when the channel is wide and water filled and when only cations or anions can permeate through the channel. Under these conditions, the entry of the ions in the channel and not the diffusion through the channel is the rate-limiting step and the Renkin correction factor (36) times the aqueous diffusion coefficient of the hydrated ions can be used to estimate the channel radius *a* from the relative permeativities of the different ions through the channel. The relative permeativities of the ions were calculated from their single-channel conductance relative to that of Rb$^+$ and plotted as a function of the hydrated ion radius *r* (51). It is noteworthy that a similar approach has been used previously to calculate the radii of porin channels from the relative rates of permeation of different solutes in the liposome swelling assay (31).

Channel size estimations from the effect of negatively charged groups at the channel. Negative charges at the opening of an ion channel result in substantial ionic strength-dependent surface potentials at the pore mouth that attract cations and repel anions. Accordingly, they influence both single-channel conductance and zero-current membrane potential. A quantitative description of the effect of the point charges on the single-channel conductance was determined using the treatment proposed previously (28, 50). These reports described the effect of point charges on the conductance of a channel, which is dependent on ion concentration, on the channel diameter, and on the number of negative charges (3). Comparison of the crystal structure of *Rhodobacter capsulatus* porin with the diameter derived from this theoretical treatment yielded good agreement (34).

Western blot analysis. In Western blot (immunoblot) experiments, the proteins separated by 10% Tricine-containing SDS-PAGE were transferred onto 0.2-μm-thick nitrocellulose sheets (Protran BA83; Schleicher & Schuell) in a semidry blotting apparatus according to a previously described method (43). This method is a modification of a previously described procedure (17) and takes into account the higher ionic strength of Tricine-containing gels. The reactive sites were blocked with 5% skim milk in Tris-buffered saline (TBS) (1 M Tris-HCl [pH 7.5], 0.01 M NaCl) for 30 min and shortly washed with three different solutions (solution 1, 1% skim milk in TBS [pH 7.5]; solution 2, 1% skim milk, 0.1% Tween in TBS [pH 7.5]; solution 3, TBS [pH 7.5]). The blots were probed for 1 h (or overnight) at room temperature with rabbit polyclonal antibodies (Charles River Wiga GmbH, Sulzfeld, Germany) raised against synthetic peptides corresponding to the N terminus of the *R. erythropolis* porin (22) in a 1:100 dilution. After the incubation, the membrane was washed with solution at a 1-to-3 ratio. Bound antibodies were detected by using horseradish-peroxidase-coupled rabbit immunoglobulins (DAKO, Glostrup, Denmark) at a 1:1,000 dilution. Color reaction was obtained after 10 min of incubation in 94% TBS–6% chloronaphthol (0.3%)–0.075% hydrogen peroxide.

RESULTS

Isolation and purification of two different channel-forming proteins of the cell wall of *R. equi*. In previous studies using organic solvents, Lichtinger et al. demonstrated that it is possible to isolate channel-forming activity from whole cells of different members of the taxon mycolata (20, 21). This is presumably possible because the cell wall channels of these organisms are deeply buried within an outer lipid layer based on MAs (and other lipids), which means that these proteins have highly hydrophobic properties (23). In this study, we extended this method to *R. equi* and investigated cells for the presence of channel-forming activities extracted using organic solvents. Proteins obtained following repeated solvent extraction and protein precipitation were subjected to single-channel conductance measurement on planar lipid bilayers. The addition of the protein resulted in a very fast reconstitution of channels and showed that the final protein precipitate contained the highest channel-forming activity. Interestingly, two different channels were identified in the reconstitution experiments, one with a high level of single-channel conductance (PorA$_{Req}$ [*R. equi* pore A]) and one with a low level of single-channel conductance (PorB$_{Req}$ [*R. equi* pore B]). The channel-forming protein PorA$_{Req}$ was isolated and purified by ice-cold ethanol precipitation of the initial diethylether-precipitated protein preparation. After centrifugation, the protein-containing pellet was dissolved in buffer containing 1% Genapol and inspected for channel-forming activity. According to the results of Tricine-containing SDS-PAGE, the major protein present had an apparent molecular mass of about 67 kDa (Fig. 1A). Identification and further purification of the channel-forming protein PorB$_{Req}$ were achieved by excision of different molecular mass bands from preparative Tricine-containing SDS-PAGE
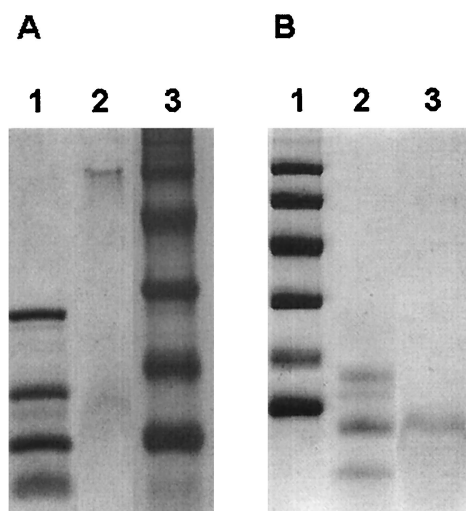
FIG. 1. SDS-PAGE of the purified cell wall channel proteins of *R. equi*. (A) PorA$_{Req}$ (*R. equi* pore A). Lane 1, molecular mass markers (26.6, 17.0, 14.2, and 6.5 kDa); lane 2, 5 μg of purified PorA$_{Req}$ solubilized at 40°C for 30 min in 20 μl of sample buffer; lane 3, molecular mass markers (94, 67, 43, 30, 20.1, and 14.4 kDa) (Coomassie blue staining). (B) PorB$_{Req}$ (*R. equi* pore B). Lane 1, molecular mass markers (94, 67, 43, 30, 20.1, and 14.4 kDa); lane 2, molecular mass markers (16.9, 14.4, 10.7, and 8.2 kDa [6.2- and 2.5-kDa molecular mass markers are not visible on the gel]); lane 3, 3 μg of purified PorB$_{Req}$ was solubilized at 40°C for 30 min in 20 μl of sample buffer (Coomassie blue staining).

and their extraction with 1% Genapol–10 mM Tris-HCl (pH 8.0). Addition of the different fractions to the black lipid bilayer demonstrated that the main channel-forming activity was present in one fraction, the major protein of which had an apparent molecular mass of about 11 kDa according to Tricine-containing SDS-PAGE (Fig. 1B).

Effect of purified PorA$_{Req}$ and PorB$_{Req}$ on the conductance of lipid bilayer membranes. We performed conductance measurements with lipid bilayer membranes from PC-PS mixtures (molar ratio, 4:1) to study the interaction of both purified cell wall channels with artificial membranes. The addition of the pure proteins at a low concentration (100 ng/ml) to one or both sides of the lipid membranes resulted in a strong increase of the conductance. The conductance increase was not sudden but was a function of time after the addition of the protein to membranes in the black state or of time after the blackening of the membranes when the protein was present in the aqueous phase before membrane formation. After about 30 min, the membrane conductance had increased by several orders of magnitude above that of membranes without the protein (from about 0.05 μS/cm^2 to more than 150 μS/cm^2). Only a small further increase (compared with the initial increase) occurred after that time. Control experiments with Genapol alone at the same concentration as used in the experiments with protein demonstrated that the membrane activity was caused by the presence of the cell wall protein and not by the detergent.

Single-channel analyses. The addition of lower concentrations of the cell wall proteins (10 ng/ml) to lipid bilayers made of PC-PS allowed the resolution of stepwise conductance increases. Figure 2 shows the results of single-channel recording in the presence of the cell wall porins PorA$_{Req}$ (panel A) and

PorB$_{Req}$ (panel B), which were added 5 min after the membrane had turned black. Shortly after the addition of the protein, the current started to increase in a step-wise fashion. Each step corresponded to the incorporation of one channel-forming unit into the membrane. Under the low-voltage conditions for the experiment whose results are depicted in Fig. 2, all the steps were directed upwards, which indicated that the channels were always in the open state and had a long lifetime (mean lifetime, more than 5 min). Figure 3 represents the histograms of the conductance fluctuations observed under the conditions described for Fig. 2. PorA$_{Req}$ had (on average) a single-channel conductance in 1 M KCl of about 4 nS (more than 45% of all conductance fluctuations) (Fig. 3A). Besides the 4-nS channel, we observed also channels with about 8 nS, as shown in Fig. 3A, which presumably represent dimers of the 4-nS channel which incorporate at the same time into the membrane. At 300 pS in 1 M KCl, the single-channel conductance of PorB$_{Req}$ was substantially smaller (more than 80% of all conductance fluctuations) (Fig. 3B). It is noteworthy that the exchange of PC-PS membranes with membranes made of other lipid mixtures such as PC alone, PC-MA (molar ratio, 4:1), or PC-MA-PS (molar ratio, 4:4:1) did not influence the single-channel conductance of either channel-forming protein.

Single-channel properties of the cell wall channels. To obtain some insight into the biophysical properties of the two cell wall channels of *R. equi*, single-channel experiments with salts containing ions other than K$^+$ and Cl$^-$ were also performed. The results summarized in Table 1 show that they indeed exhibited different channel characteristics. Cations had a strong influence on the single-channel conductance of PorA$_{Req}$, leading to the conclusion that the cell wall channel is cation selective. The ionic selectivity of PorA$_{Req}$ for cations was K$^+$ ≈ Rb$^+$ ≈ Cs$^+$ > Na$^+$ > Li$^+$ > Tris$^+$, which means that the
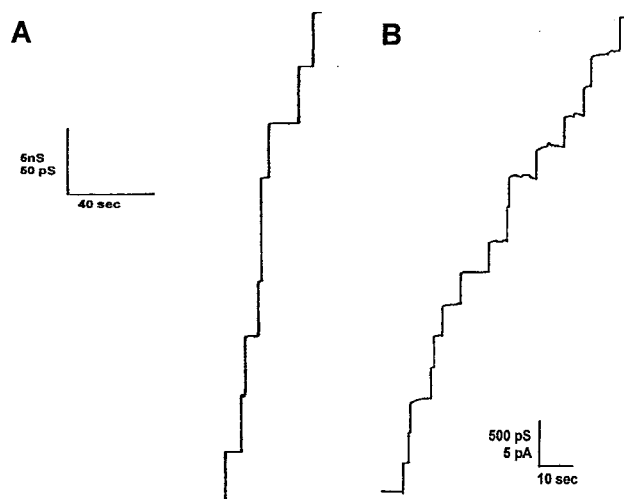

FIG. 2. Single-channel recordings of a PC–PS (molar ratio 4:1)–*n*-decane membrane in the presence of the purified cell wall channels of *R. equi*. In both cases, the aqueous phase contained 1 M KCl, 10 mM Tris-HCl (pH 8.0), and 10 ng of cell wall protein/ml. The applied membrane potential was 10 mV, and the temperature was 20°C. (A) Recording of PorA$_{Req}$, the 67-kDa protein from the cell wall of *R. equi*. (B) Recording of PorB$_{Req}$, the 11-kDa protein from the cell wall of *R. equi*.
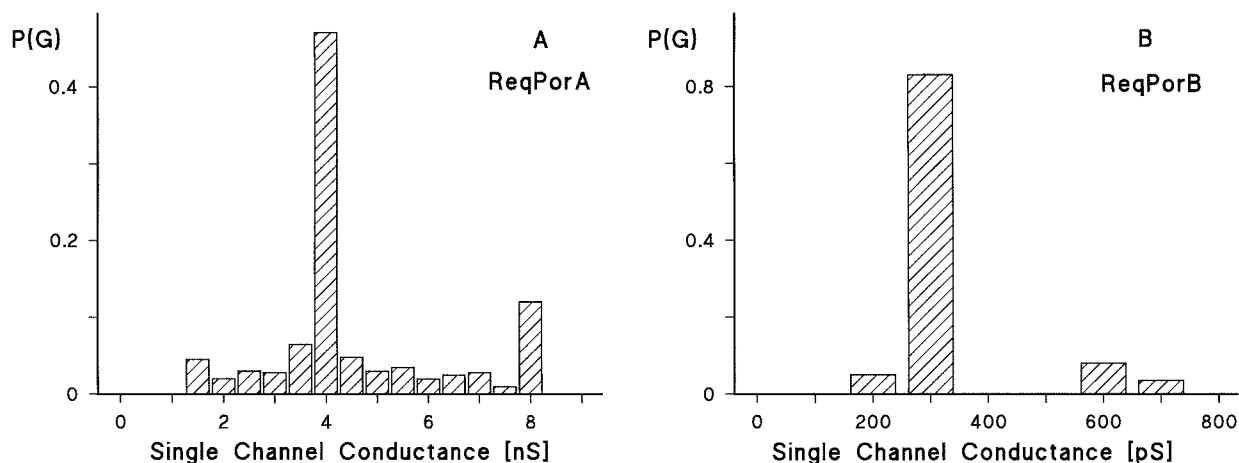
FIG. 3. Histograms of the probability $P(G)$ for the occurrence of a given conductivity unit observed with membranes formed of PC–PS (molar ratio 4:1)–*n*-decane in the presence of the cell wall channels of *R. equi*. $P(G)$ is the probability that a given conductance increment G is observed in the single-channel experiments. It was calculated by dividing the number of fluctuations with a given conductance increment by the total number of conductance fluctuations. The aqueous phase contained 1 M KCl and 10 mM Tris-HCl (pH 8.0). The applied membrane potential was 10 mV, and the temperature was 20°C. (A) Histogram after addition of $PorA_{Req}$. The average single-channel conductance for 109 single-channel events was 4 nS. (B) Histogram after addition of $PorB_{Req}$. The average single-channel conductance for 121 single-channel events was 300 pS.

permeability of the cations through the channels approximately followed their mobility sequence in the aqueous phase. This result suggests that $PorA_{Req}$ forms a wide and water-filled channel. In contrast, the single-channel conductance of $PorB_{Req}$ was much less dependent on the type of cation present in the aqueous solution than that of $PorA_{Req}$. This result indicated that $PorB_{Req}$ is anion selective, a reasonable assumption in that a second cation-selective channel of small permeability would be unnecessary given the presence of the highly conductive $PorA_{Req}$.

Table 1 also shows G, the average single-channel conductance, as a function of the KCl concentration in the aqueous phase. Measurements were performed down to 0.01 M KCl. As for other cell wall channels of the mycolata (20, 39, 40, 50), we did not observe a linear relationship between single-channel conductance and KCl concentration for $PorA_{Req}$ or $PorB_{Req}$. This would in principle be expected for wide water-filled channels similar to those formed by general diffusion channels of gram-negative bacteria (2, 53). Instead, the single-channel conductance G was proportional to the square root of the concentration, because the conductance of both cell wall channels increased by a factor of only about 10 for a 100-fold increase of the salt concentration (Table 1). This indicated point charge affects the channel properties of $PorA_{Req}$ and $PorB_{Req}$, i.e., their selectivity is caused by charged groups in or near the channel mouth (see Discussion). It is noteworthy that the charge effects were caused by charges attached to the channel and not by the negatively charged lipids present in the membrane. This was determined from the observation that the cell wall porin had the same conductance in neutral (pure PC) and in negatively charged membranes (PC-PS, PC-MA, and PC-MA-PS).

Selectivity of the cell wall channels of *R. equi*. We performed zero-current membrane potential measurements to obtain further information on the molecular structure of the cell wall channels of *R. equi*. After incorporation of 100 to 1,000 channels into the PC-PS membranes, the salt concentration on one

side of the membranes was raised fivefold (beginning at 100 mM), and the zero-current potential was measured 5 min after every increase of the salt gradient across the membrane. For $PorA_{Req}$, with all three salts employed in these experiments (KCl, LiCl, and KCH_3COO), the more dilute side of the membrane (100 mM) always became positive (Table 2), which indicated preferential movement of the cations through the channel; i.e., this cell wall channel is cation selective, as was

TABLE 1. Average single-channel conductance G of the cell wall channels $PorA_{Req}$ and $PorB_{Req}$ of *R. equi* in different salt solutions[a]

Salt	Concn (M)	G (nS) for:	
		$PorA_{Req}$	$PorB_{Req}$
LiCl	1.0	2.00	0.300
NaCl	1.0	2.50	0.250
KCl	0.01	0.20	0.025
KCl	0.03	0.35	0.070
KCl	0.1	0.75	0.100
KCl	0.3	1.50	0.175
KCl	0.6	3.00	0.225
KCl	1.0	4.00	0.300
KCl	3.0	7.00	0.850
RbCl	1.0	4.00	0.300
CsCl	1.0	4.00	0.275
NH_4Cl	1.0	4.00	0.300
$N(CH_3)_4Cl$	1.0	2.20	0.200
$N(C_2H_5)_4Cl$	1.0	0.50	0.125
Tris Cl (pH 6)	1.0	0.35	0.100
KCH_3COO	1.0	3.50	0.125
KNO_3	1.0	NM^b	0.250
KBr	1.0	NM	0.300
KF	1.0	NM	0.175

[a] The membranes were formed of PC–PS (molar ratio, 4:1) dissolved in *n*-decane. The aqueous solutions were buffered with 10 mM Tris-HCl and had a pH of 8 unless otherwise indicated. The applied voltage was 10 mV for measurements of $PorA_{Req}$ and 20 mV for measurements of $PorB_{Req}$. The temperature was 20°C. Average single-channel conductance G was calculated from at least 80 single events.

[b] NM, not measured.

TABLE 2. Zero-current membrane potentials V_m of PC–PS (molar ratio, 4:1)–n-decane membranes in the presence of the cell wall channels $PorA_{Req}$ and $PorB_{Req}$ of $R.$ $equi$ measured for a fivefold gradient of different salts[a]

Salt	Zero-current membrane potentials and P_{cation} and P_{anion} permeability ratios for:			
	$PorA_{Req}$		$PorB_{Req}$	
	V_m/mV	P_{cation}/P_{anion}	V_m/mV	P_{cation}/P_{anion}
KCl	+27	9.0	−27	0.16
LiCl	+28	8.2	−29	0.13
KCH$_3$COO	+31	8.5	−29	0.13

[a] V_m is defined as the difference between the potential at the dilute side (100 mM) and the potential at the concentrated side (500 mM). The aqueous salt solutions were buffered with 10 mM Tris-HCl, pH 8; the temperature was 20°C. The permeability ratio P_{cation}/P_{anion} was calculated using the Goldman-Hodgkin-Katz equation (6) from at least 3 individual experiments.

already suggested from the single-channel recordings (Table 1). Using the Goldman-Hodgkin-Katz equation (6), analysis of the zero-current potentials suggested that anions also might have limited permeability through the channel, because the ratios of permeability of P_{cation} and P_{anion} were 8.2 (LiCl), 9.00 (KCl), and 8.5 (potassium acetate). On the other hand, the permeability ratios are close to one another, which is unexpected for moderately selective channels such as the general diffusion pores of gram-negative bacteria because of the different mobilities of anions and cations in a wide water-filled channel (4).

The data of Table 1 demonstrate clearly that the channel formed by $PorB_{Req}$ is anion selective, because the more dilute side of the membrane has a negative zero-current membrane potential. The asymmetry potentials for the three salts used in the experiments were again very close together, which suggests that the channel properties of $PorB_{Req}$ are also controlled by point charges which are positive. Analysis of the zero-current membrane potentials using the Goldman-Hodgkin-Katz equation (5) yielded permeability ratios that are between 6 and 8 for anions over cations, again with little difference for the three salts. Taken together, these results indicate that the two channels are ideally selective, although the Nernst limit of the zero-current membrane potential is not reached. Point charges change the ion concentration near the channel with respect to that of the bulk aqueous phase, which means that the maximum potential cannot be reached.

The two cell wall channels have different voltage dependences. In single-channel recordings, the cell wall porin $PorA_{Req}$ exhibited some flickering at higher voltages; i.e., it showed rapid transitions between open and closed configurations. This might have been caused by voltage-dependent closing of $PorA_{Req}$; therefore, we measured the voltage dependence of the channel in multichannel experiments. Figure 4 shows an example of these measurement for voltages between ±10 and ±30 mV. For positive and negative applied voltages, the potential decreased in an exponential fashion (Fig. 4), similar to previous observations for the cell wall channels of $N.$ $corynebacteroides,$ $R.$ $erythropolis,$ and $C.$ $glutamicum$ (20, 22, 37). Interestingly, we observed a symmetric response for voltages between ±10 mV and ±120 mV independently of whether we added the porin at the cis side, at the $trans$ side, or at both sides of the membrane (Fig. 5). These results indicated
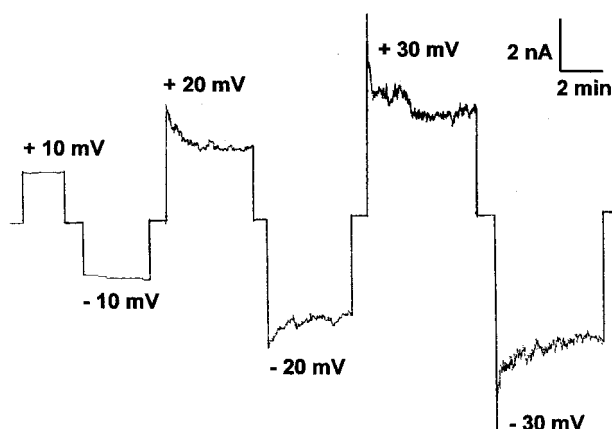

FIG. 4. Study of the voltage gating of the cation-selective cell wall channel $PorA_{Req}$. Cell wall channel protein (500 ng/ml) was added to the cis side of a black PC–PS (molar ratio, 4:1)–n-decane membrane, and the reconstitution of the channels was monitored for about 30 min. When about 100 channels were reconstituted into the membrane, increasing positive (upper traces) and negative voltages (lower traces) were applied to the cis side of the membrane and the membrane current was measured as a function of time. The aqueous phase contained 1 M KCl and 10 mM Tris-HCl (pH 8.0), and the temperature was 20°C.

either a random orientation of the porin $PorA_{Req}$ or a symmetric response to the applied voltage. In contrast, $PorB_{Req}$ was found not to be voltage gated (at least up to about ±100 mV) when the channel-forming protein was added to one or both sides of black PC–PS–n-decane membranes (Fig. 5). This
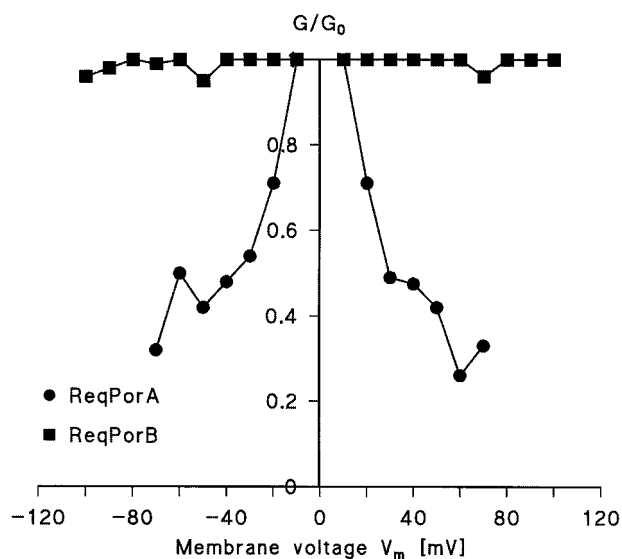

FIG. 5. Ratio of the conductance G at a given membrane potential (V_m) divided by the conductance G_o at 10-mV membrane potential as a function of membrane potential V_m measured for $PorA_{Req}$ and $PorB_{Req}$. The circles indicate measurements determined when $PorA_{Req}$ was added to the cis side of the membranes, and the squares indicate measurements determined when $PorB_{Req}$ was added to the same side of the membranes. The aqueous phase contained 1 M KCl, 10 mM Tris-HCl (pH 8.0), and 100 ng of protein/ml. The membranes were formed from PC-PS (molar ratio, 4:1) dissolved in n-decane. The temperature was 20°C. Mean values for at least four experiments are shown.
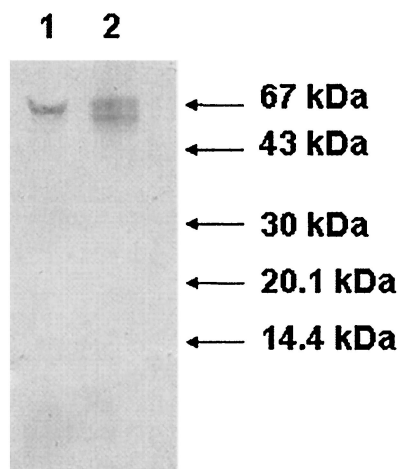
FIG. 6. Western blot analysis (using polyclonal antibody to the *R. erythropolis* porin) of the cell wall porins of *R. erythropolis* and *R. equi*. Positions of size markers are shown on the right. The channel-forming protein $PorA_{Req}$ was extracted as described in Materials and Methods, and the cell wall channel of *R. erythropolis* was determined as described previously (22). Lane 1, cation-selective channel-forming protein of *R. equi* ($PorA_{Req}$); lane 2, channel-forming protein of *R. erythropolis*.

means that the two cell wall channels responded differently to applied voltage.

Western blot assays. A channel-forming protein (porin) with a low molecular mass has recently been characterized in *R. erythropolis* (22). We performed Western blot analysis using a polyclonal rabbit antibody against a polypeptide derived from the *R. erythropolis* porin. The antibody reacted strongly with the 67-kDa polypeptide band of the $PorA_{Req}$ porin and the postulated oligomer of *R. erythropolis*, which we used as a control (Fig. 6). Furthermore, the antibody detected clearly the 11-kDa porin $PorB_{Req}$ of *R. equi* (data not shown). However, the 11-kDa porin $PorB_{Req}$ of *R. equi* did not cross-react strongly with either of two commercially available hyperimmune sera prepared for passive immunization for the protection of foals against *R. equi* infection (data not shown).

DISCUSSION

The asymmetric outer lipid layer described in current models of the cell envelopes of the mycolata (8, 10, 15, 32, 35, 48) is predicted to act as a permeability barrier against hydrophilic compounds in a similar manner to the outer membrane of gram-negative bacteria (4). The presence of this permeability barrier suggests the need for water-filled channels (porins) providing a pathway through the outer lipid layer. Consistent with this prediction, the results presented herein confirm that the cell envelope of *R. equi* contains at least two distinct organic solvent-extractable channel-forming proteins with complementary selectivities for anions and cations. Both types of channel are presumably also capable of transporting neutral solutes of sizes below the molecular weight cutoffs determined by their respective internal diameters (see below).

The cation-selective channel $PorA_{Req}$ had a single-channel conductance of 4 nS in 1 M KCl and was voltage gated. Experiments with higher membrane potentials suggested that its voltage gating is symmetric and that the symmetry is indepen-

dent of whether we added the channel-forming protein to one side of the membrane or to both sides. Starting at about ±20 mV, the channels closed, and the application of ±40 mV led to a closure of 50% of all channels in the membrane. These results indicated either that the protein was reconstituted in a random conformation in the membrane or that the channels reacted symmetrically to the applied membrane voltage. It is noteworthy that voltage dependence has been found for many cell wall channels. Some of them showed asymmetric voltage-dependent gating; the channels closed only when the *cis* side (the side with the addition of the protein) had negative voltage, as observed for channels from *C. glutamicum* (20), *N. corynebacteroides* (37), and *R. erythropolis* (22). Moreover, a proportion of these channels seemed to close irreversibly after the application of ±50 mV and higher voltages, which means that the potential at the inner side of the cell wall might influence their permeability properties. The potential might come from a Donnan potential across the cell wall, as has been observed in *Escherichia coli* cells (44). However, it is also possible that the function of $PorA_{Req}$ in vivo is unaffected by the potential difference across the MA permeability barrier. It is noteworthy that $PorB_{Req}$ was not voltage gated. $PorA_{Req}$ has an apparent molecular mass of 67 kDa by SDS-PAGE and we did not observe dissociation of the 67-kDa protein after boiling. The calculated pore diameter (1.8 to 2.0 nm) of $PorA_{Req}$ is somewhat smaller than those calculated for the porins of *R. erythropolis* (22), *N. corynebacteroides* (37), and *C. glutamicum* (20), consistent with the observation that the conductance of the *R. equi* channel is lower than those of the other cell wall porins in the same salt solutions (Table 3).

The anion-selective channel $PorB_{Req}$ showed a much lower channel conductance in 1 M KCl of 300 pS and is not voltage gated. This means the channel acts like a diffusion pore which is specialized for anions and that the limiting step for the transport through this channel is likely to be the charge and the molecular mass of the molecule itself. This result is in agreement with the anion-selective cell wall channel of *M. bovis*, which is also not voltage gated and which has also a much smaller single-channel conductance than the cation-selective cell wall channel of the same organism (21). $PorB_{Req}$ has an apparent molecular mass of about 11 kDa, but a single polypeptide is presumably too small to account for such a big channel, which means that the channel is presumably formed by an oligomer. After boiling of $PorB_{Req}$, we observed no change in molecular mass, suggesting that the channel is most likely composed of 11-kDa subunits. This is comparable to the situation for *R. erythropolis*, in which the channel, which has a diameter of about 2.0 nm, is formed by a small, 8.4-kDa subunit (22).

Gram-negative bacteria contain four classes of outer membrane channels reflecting different strategies for the passage of hydrophilic compounds through their outer membranes. General diffusion porins form water-filled channels for the nonspecific diffusion of hydrophilic compounds, whereas specific porins contain binding sites for classes of particular solutes. In addition, receptors and efflux channels may also be present (4). The properties of the cell wall channels $PorA_{Req}$ and $PorB_{Req}$ are similar to those found in the cell walls of closely related MA-containing actinomycetes (Table 3). Thus, in species representing four major genera of the mycolata, we have identified

TABLE 3. Comparison of the cell wall channel properties of *R. equi, R. erythropolis, C. glutamicum, N. farcinica, N. corynebacteroides*
(*R. corynebacteroides*) and *M. bovis* BCG

Cell wall porin of indicated species	G (nS) in 1 M KCl	Selectivity $(P_c/P_a)^a$ in KCl	Point charges at the channel mouth	Channel diameter (nm) by ion radius[b]	Channel diameter (nm) by negative point charge[c]	Reference or source
R. equi						
$PorA_{Req}$	4.00	9.0	−1.5	1.8	2.0	This study
$PorB_{Req}$	0.30	0.16	+1.5	1.4	1.4	
R. erythropolis	6.00	11.80	−2.7	2.0	2.0	22
C. glutamicum PorA	5.50	8.10	−2.0	2.2	2.2	20
N. corynebacteroides (*R. corynebacteroides*)	5.50	3.80	−2.7	2.0	2.2	37
N. farcinica	3.0	8.2	−1.3	1.4	1.6	40
M. bovis BCG						21
$PorA_{Mbo}$	4.30	>1	ND[d]	ND	ND	
$PorB_{Mbo}$	0.78	<1	ND	ND	ND	

[a] P_c/P_a, P_{cation}/P_{anion}.
[b] Estimated from the single-channel conductance as a function of the hydrated ion radii.
[c] Estimated from the effect of negative point charges on single-channel conductance.
[d] ND, not done.

so far only specialized (i.e., channels containing point-negative net charges) but nonspecific pore-forming proteins. Common to this class of porins is that they are wide and water filled and that they contain charges at the channel mouth. Most cell wall channels contain negative point charges. However, it is noteworthy that one other anion-selective channel has been found previously in *M. bovis* besides a high-conductance cation-selective pore (21), similar to the situation described here for *R. equi*. The evolution of two protein channels with distinctive features may be a conserved and general principle in the cell wall channels of MA-containing actinomycetes. We presume that the distribution of anion-selective channels in the mycolata will match that of the cation-selective channels to facilitate the uptake of both kinds of solutes. Cation-selective channels may be more abundant in the cell envelope, making them easier to detect and isolate. However, it is noted that anion-selective pore-forming proteins appear to be less frequent than cation-selective pore-forming proteins in gram-negative bacteria (7). In addition to those described above, channel-forming proteins have recently been identified in the more distantly related actinomycetes that lack MAs but presumably present some kind of as-yet-undescribed cell wall permeability barrier (18, 19). However, the wall channel of *Streptomyces griseus* is distinctive in that it contains a binding site for the antibiotic streptomycin, which is produced by that organism (18), while that of *Micromonospora purpurea* is apparently a substantially larger, 200-kDa protein with unusually high (14 nS) single-channel conductance (19).

The diameter of the $PorA_{Req}$ channel of *R. equi* was estimated on the basis of its single-channel conductance (51). The estimation used the relative permeability of the different cations through the channel, as calculated from the single-channel conductance. This means that it was based on the same assumptions which have been used previously for the derivation of the Renkin equation (36) for the diffusion of neutral molecules through porous membranes (see Experimental Procedures in that report). Figure 7 shows the fit of the relative permeability of the $PorA_{Req}$ channel for cations with the Renkin equation (equation 6 of reference 51) times the aqueous diffusion coefficient of the ions as a function of the hydrated

radii calculated from the limiting molar conductivity of the cations by using Stoke's equation (taken from reference 51). The data points are given relative to the data for Rb^+, the cation with the smallest hydrated ion radius, whose value was set to unity, and the best fit of the relative permeability was obtained with $r = 0.9$ nm (Fig. 7; diameter, 1.8 nm). A diameter of 1.8 nm is very similar to those of cell wall channels from other mycolata despite a different molecular mass of the channel-forming proteins (Table 3). The data of $PorB_{Req}$ could not be analyzed using the Renkin formula, because the anions seem to interact with the channel and because the relative
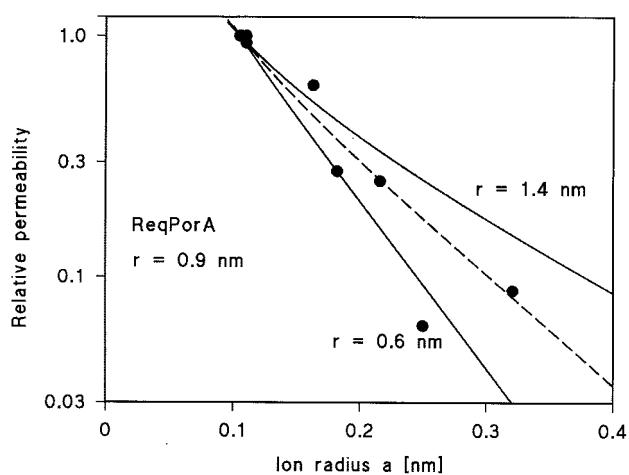
FIG. 7. Fit of the single-channel conductance data of the cell wall channel $PorA_{Req}$ as determined by multiplying the Renkin correction factor by the aqueous diffusion coefficients of the different cations. The product of the two numbers was normalized to 1 for $a = 0.105$ nm (Rb^+). Single-channel conductances were normalized to the ones of Rb^+ and plotted versus the hydrated ion radii taken from reference 50. The closed points correspond to Li^+, Na^+, K^+, NH_4^+, Cs^+, $N(CH_3)_4^+$, $N(C_2H_5)_4^+$ and $Tris^+$, which were all used for the pore-diameter estimation (see Discussion). The fit (solid lines) is shown for $r = 1.4$ nm (upper line) and $r = 0.6$ nm (lower line). The best fit was achieved with $r = 0.9$ nm (diameter = 1.8 nm), which corresponds to the broken line.
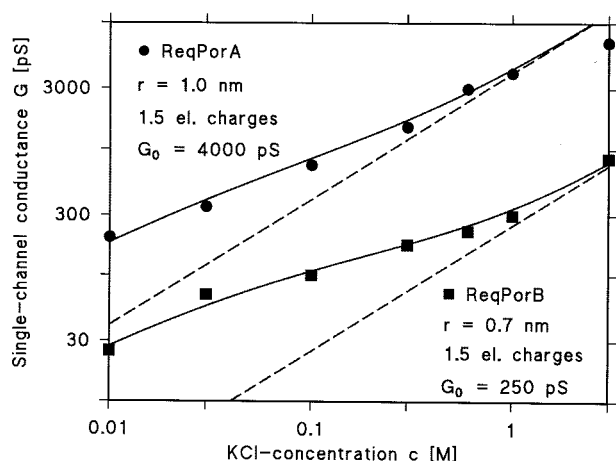
FIG. 8. Single-channel conductance of the cell wall channels of *R. equi* as a function of the KCl concentration in the aqueous phase. Conductances are shown as circles (PorA$_{Req}$) and squares (PorB$_{Req}$). The solid lines represent the fit of the single-channel conductance data with the Nelson and McQuarrie formula (equations 1 to 6 of reference 49), assuming the presence of negative and positive point charges (1.5 positive charges) at the channel mouth and assuming channel diameters of 2 nm (PorA$_{Req}$) and 1.4 nm (PorB$_{Req}$). c, molar concentration of the KCl solution; G, average single-channel conductance in pS (10^{-12} S). The broken (straight) lines show the single-channel conductances of the two cell wall channels when no point charges are present and correspond to linear functions between channel conductance and bulk aqueous salt concentration.

permeability of the channel differed only little for the different anions.

For each channel-forming activity, the single-channel conductance was not saturable at high salt concentration and the conductance was not a linear function of the bulk aqueous concentration (Table 1). For both channels, we observed an increase of the single-channel conductance of about three- to fivefold for an increase of the KCl concentration by a factor of 10. This means that (i) ion selectivity is not related to the presence of a binding site and that (ii) point charges are involved in ion selectivity, as we have demonstrated previously for other porins of the mycolata (37, 40, 50). We analyzed the single-channel conductance derived in this study by using equations 1 to 6 of a previous study (50). Assuming that the PorA$_{Req}$ channel has a diameter of 2.0 nm and that 1.5 negative point charges ($[q] = -2.4 \times 10^{-19}$ A $\times$ s) are attached to the channel mouth, we received a reasonable fit of the data (Fig. 8). We analyzed the data of PorB$_{Req}$ with the same formula and, assuming a channel diameter of 1.4 nm and the presence of 1.5 positive point charges ($q = +2.4 \times 10^{-19}$ A $\times$ s) in or near the channel mouth, derived the fit (Fig. 8). We used concentrations for the fits instead of activities, since single-channel conductance of general diffusion channels from bacterial outer membranes is a linear function of bulk aqueous conductivity (2). Furthermore, it is not yet known whether concentrations or activities best describe the conditions on a membrane surface. The fit of the experimental data with the previously proposed formula (50) was less satisfactory at high salt concentrations (3 M) than at low salt concentrations (0.01 to 1 M). It is noteworthy that the potential at the mouth of the channel (negative in the case of PorA$_{Req}$ and positive in the

case of PorB$_{Req}$) has important implications for the function of the cell wall channels. Under physiological conditions and due to the presence of a selectivity filter, increasing concentrations of counter-ions at the channel mouth cause the channel to preferentially conduct anions or cations without being truly selective.

Southern blot analyses indicate that the mycolata contain conserved gene sequences for porins in their chromosomes (23, 38). Consistent with this, we observed cross-reactions between the porin channels of *R. equi* and a polyclonal antibody raised against the *R. erythropolis* cation-selective channel, which shows similar properties to that of PorA$_{Req}$ (Table 3). However, N-terminal sequence analysis of a preparation of PorA$_{Req}$ yielded a sequence which is distinct from that of the *R. erythropolis* cation-selective channel (data not shown). The amino acid sequence available for this rhodococcal cell wall channel and the known sequences of cell wall channels of the mycolata that have been characterized (23, 30, 45) are all distinct from each other, suggesting that these proteins belong to several different protein families (41). The pathogenic mycolata, such as *R. equi* and *M. tuberculosis*, typically survive as intracellular pathogens within granulomatous lesions in their hosts and as such are inaccessible to many standard antibiotics. The difficulty presented by this barrier to effective treatment is further compounded by the presence of the lipid-rich outer permeability barrier in the cell envelopes of these bacteria. Therefore, understanding the properties of their channel-forming proteins may help to put the antimicrobial susceptibility patterns of the mycolata into context and may aid in the design of novel therapeutics.

REFERENCES

1. **Andersen, S. J., S. Quan, B. Gowan, and E. R. Dabbs.** 1997. Monooxygenase-like sequence of a *Rhodococcus equi* gene conferring increased resistance to rifampin by inactivating this antibiotic. Antimicrob. Agents Chemother. **41:** 218–221.
2. **Benz, R.** 1988. Structure and function of porins from gram-negative bacteria. Annu. Rev. Microbiol. **42:**359–393.
3. **Benz, R.** 1994. Solute uptake through bacterial outer membrane, p. 397–423. *In* J.-M. Ghuysen and R. Hakenbeck (ed.), Bacterial cell wall. Elsevier Science B.V., Amsterdam, The Netherlands.
4. **Benz, R.** 2001. Porins—structure and function, p. 227–246. *In* G. Winkelmann (ed.), Microbial transport systems. Wiley-VCH Verlag GmbH, Weinheim, Germany.
5. **Benz, R., K. Janko, W. Boos, and P. Läuger.** 1978. Formation of large ion-permeable membrane channels by the matrix protein (porin) of *Escherichia coli*. Biochim. Biophys. Acta **511:**305–319.
6. **Benz, R., K. Janko, and P. Läuger.** 1979. Ionic selectivity of pores formed by the matrix protein (porin) of *Escherichia coli*. Biochim. Biophys. Acta **551:** 238–247.
7. **Benz, R., A. Schmid, and R. E. W. Hancock.** 1985. Ion selectivity of gram-negative bacterial porins. J. Bacteriol. **162:**722–727.
8. **Brennan, P. J., and H. Nikaido.** 1995. The envelope of mycobacteria. Annu. Rev. Biochem. **64:**29–63.
9. **Chun, J., S.-O. Kang, Y. C. Hah, and M. Goodfellow.** 1996. Phylogeny of mycolic acid-containing actinomycetes. J. Ind. Microbiol. **17:**205–213.
10. **Dmetriev, B. A., S. Ehlers, E. T. Rietschel, and P. J. Brennan.** 2000. Molecular mechanics of the mycobacterial cell wall: from horizontal layers to vertical scaffolds. Int. J. Med. Microbiol. **290:**251–258.
11. **Erhardt, W., V. Neuhoff, N. Arnold, and D. Taube.** 1988. Improved staining

of proteins in polyacrylamide gels including isoelectric focusing gels with clear background at nanogram sensitivity using CBB G-250 and R-250. Electrophoresis **9:**255–262.

12. **Fines, M., S. Pronost, K. Maillard, S. Taouji, and R. LeClercq.** 2001. Characterization of mutations within the *rpoB* gene associated with rifampin resistance in *Rhodococcus equi* isolated from foals. J. Clin. Microbiol. **39:** 2784–2787.

13. **Giguère, S., and J. F. Prescott.** 1997. Clinical manifestations, diagnosis, treatment and prevention of *Rhodococcus equi* infections in foals. Vet. Microbiol. **56:**313–334.

14. **Golub, B., G. Falk, and W. W. Spink.** 1967. Lung abscess due to *Corynebacterium equi*. Report of first human infection. Ann. Intern. Med. **66:**1174–1177.

15. **Jarlier, V., and H. Nikaido.** 1990. Permeability barrier to hydrophilic solutes in *Mycobacterium chelonae*. J. Bacteriol. **172:**1418–1423.

16. **Kartmann, B., S. Stenger, and M. Niederweis.** 1999. Porins in the cell wall of *Mycobacterium tuberculosis*. J. Bacteriol. **181:**6543–6546.

17. **Khyse-Anderson, J.** 1984. Electroblotting of multiple gels: a simple apparatus without buffer tank for rapid transfer of proteins from polyacrylamide to nitrocellulose. J. Biochem. Biophys. Methods **10:**203–209.

18. **Kim, B.-H., C. Andersen, and R. Benz.** 2001. Identification of a cell wall channel of *Streptomyces griseus*: the channel contains a binding site for streptomycin. Mol. Microbiol. **41:**665–673.

19. **Kim, B.-H., K. Wengerter, and R. Benz.** 2002. The cell wall of *Micromonospora purpurea* contains a high conductance channel. Arch. Microbiol. **177:** 184–191.

20. **Lichtinger, T., A. Burkovski, M. Niederweis, R. Krämer, and R. Benz.** 1998. Biochemical and biophysical characterization of the cell wall channel of *Corynebacterium glutamicum*: the channel is formed by a low molecular mass subunit. Biochemistry **37:**15024–15032.

21. **Lichtinger, T., B. Heym, E. Maier, H. Eichner, S. T. Cole, and R. Benz.** 1999. Evidence for a small anion-selective channel in the cell wall of *Mycobacterium bovis* BCG besides a wide cation-selective pore. FEBS Lett. **454:**349–355.

22. **Lichtinger, T., G. Reiss, and R. Benz.** 2000. Biochemical identification and biophysical characterization of a channel-forming protein from *Rhodococcus erythropolis*. J. Bacteriol. **182:**764–770.

23. **Lichtinger, T., F. G. Rieß, A. Burkovski, F. Engelbrecht, D. Hesse, H. Kratzin, R. Krämer, and R. Benz.** 2001. The low-molecular-mass subunit of the cell wall channel of the Gram-positive *Corynebacterium glutamicum*. Immunological localization, cloning and sequencing of its gene *porA*. Eur. J. Biochem. **268:**462–469.

24. **Minnikin, D. E.** 1982. Lipids: complex lipids, their chemistry, biosynthesis and roles, p. 95–184. *In* C. Ratledge and J. L. Stanford (ed.), The biology of the mycobacteria. Academic Press, London, United Kingdom.

25. **Mosser, D. M., and M. K. Hondalus.** 1996. *Rhodococcus equi*: an emerging opportunistic pathogen. Trends Microbiol. **4:**29–33.

26. **Mukhopadhyay, S., D. Basu, and P. Chakrabarti.** 1997. Characterization of a porin from *Mycobacterium smegmatis*. J. Bacteriol. **179:**6205–6207.

27. **Munoz, P., A. Burillo, J. Palomo, M. Rodriguez-Creixems, and E. Bouza.** 1998. *Rhodococcus equi* infection in transplant recipients: case report and review of the literature. Transplantation **65:**449–453.

28. **Nelson, A. P., and D. A. McQuarrie.** 1975. The effect of discrete charges on the electrical properties of the membrane. J. Theor. Biol. **55:**13–27.

29. **Niederweis, M., E. Maier, T. Lichtinger, R. Benz, and R. Krämer.** 1995. Identification of channel-forming activity in the cell wall of *Corynebacterium glutamicum*. J. Bacteriol. **177:**5716–5718.

30. **Niederweis, M., S. Ehrt, C. Heinz, U. Klöcker, S. Karosi, K. M. Swiderek, L. W. Riley, and R. Benz.** 1999. Cloning of the mspA gene encoding a porin from *Mycobacterium smegmatis*. Mol. Microbiol. **33:**933–945.

31. **Nikaido, H., and E. Y. Rosenberg.** 1981. Effect of solute size on diffusion rates through the transmembrane pores of the outer membrane of *Escherichia coli*. J. Gen. Physiol. **77:**121–135.

32. **Nikaido, H., S. H. Kim, and E. Y. Rosenberg.** 1993. Physical organization of lipids in the cell wall of *Mycobacterium chelonae*. Mol. Microbiol. **8:**1025–1030.

33. **Prescott, J. F.** 1991. *Rhodococcus equi*: an animal and human pathogen. Clin. Microbiol. Rev. **4:**20–34.

34. **Przybylski, M., M. O. Glocker, U. Nestel, V. Schnaible, K. Diederichs, J. Weckesser, M. Schad, A. Schmid, W. Welte, and R. Benz.** 1996. X-ray crystallographic and mass spectrometric structure determination and functional characterization of succinylated porin from *Rhodobacter capsulatus*: implications for ion selectivity and single-channel conductance. Protein Sci. **5:**1477–1489.

35. **Puech, V., M. Chami, A. Lemassu, M.-A. Lanélle, B. Schiffler, P. Gounon, N. Bayan, R. Benz, and M. Daffé.** 2001. Structure of the cell envelope of corynebacteria: importance of the non-covalently bound lipids in the formation of the cell wall permeability barrier and fracture plane. Microbiology **147:**1365–1382.

36. **Renkin, E. M.** 1954. Filtration, diffusion, and molecular sieving through porous cellulose membranes. J. Gen. Physiol. **38:**225–243.

37. **Rieß, F. G., and R. Benz.** 2000. Discovery of a novel channel-forming protein in the cell wall of the non-pathogenic *Nocardia corynebacteroides*. Biochim. Biophys. Acta **1509:**485–495.

38. **Rieß, F. G., U. Dörner, B. Schiffler, and R. Benz.** 2001. Study of the properties of a channel forming protein of the cell wall of the gram-positive bacterium *Mycobacterium phlei*. J. Membr. Biol. **182:**147–157.

39. **Rieß, F. G., T. Lichtinger, A. F. Yassin, K. P. Schaal, and R. Benz.** 1999. The cell wall porin of the gram-positive bacterium *Nocardia asteroides* forms cation-selective channels that exhibit asymmetric voltage dependence. Arch. Microbiol. **171:**173–182.

40. **Rieß, F. G., T. Lichtinger, R. Cseh, A. F. Yassin, K. P. Schaal, and R. Benz.** 1998. The cell wall channel of *Nocardia farcinica*: biochemical identification of the channel-forming protein and biophysical characterization of the channel properties. Mol. Microbiol. **29:**139–150.

41. **Saier, M. H.** 2000. A functional-phylogenetic classification system for transmembrane solute transporters. Microbiol. Mol. Biol. Rev. **64:**354–411.

42. **Schäger, H., and G. von Jagow.** 1987. Tricine-sodium dodecyl sulfate-polyacrylamide gel electrophoresis for the separation of proteins in the range from 1 to 100 kDa. Anal. Biochem. **166:**368–379.

43. **Schäger, H., and G. von Jagow.** 1991. Blue native electrophoresis for isolation of membrane protein complexes in enzymatically active form. Anal. Biochem. **199:**223–231.

44. **Sen, K., J. Hellman, and H. Nikaido.** 1988. Porin channels in intact cells of *Escherichia coli* are not affected by Donnan potentials across the outer membrane. J. Biol. Chem. **263:**1182–1187.

45. **Senaratne, R. H., H. Mobasheri, K. G. Papavinasasundaram, P. Jenner, E. J. A. Lea, and P. Draper.** 1998. Expression of a gene for a porin-like protein of the OmpA family from *Mycobacterium tuberculosis* H37Rv. J. Bacteriol. **180:**3541–3547.

46. **Stratton-Phelps, M., W. D. Wilson, and I. A. Gardner.** 2000. Risk of adverse effects in pneumonic foals treated with erythromycin versus other antibiotics: 143 cases (1986–1996). J. Am. Vet. Med. Assoc. **217:**68–73.

47. **Sutcliffe, I. C.** 1997. Macroamphiphilic cell envelope components of *Rhodococcus equi* and closely related bacteria. Vet. Microbiol. **56:**287–299.

48. **Sutcliffe, I. C.** 1998. Cell envelope composition and organization in the genus *Rhodococcus*. Antonie Leeuwenhoek **74:**49–58.

49. **Takai, S., K. Takeda, Y. Nakano, T. Karasawa, J. Furugoori, Y. Sasaki, S. Tsubaki, T. Higuchi, T. Anzai, R. Wada, and M. Kamada.** 1997. Emergence of rifampin-resistant *Rhodococcus equi* in an infected foal. J. Clin. Microbiol. **35:**1904–1908.

50. **Trias, J., and R. Benz.** 1993. Characterization of the channel formed by the mycobacterial porin in lipid bilayer membranes. Demonstration of voltage gating and of negative point charges at the channel mouth. J. Biol. Chem. **268:**6234–6240.

51. **Trias, J., and R. Benz.** 1994. Permeability of the cell wall of *Mycobacterium smegmatis*. Mol. Microbiol. **14:**283–290.

52. **Weinstock, D. M., and A. E. Brown.** 2002. *Rhodococcus equi*: an emerging pathogen. Clin. Infect. Dis. **34:**1379–1385.

53. **Weiss, M. S., A. Kreusch, E. Schlitz, U. Nestel, W. Welte, J. Weckesser, and G. E. Schultz.** 1991. The structure of porin from *Rhodobacter capsulatus* at 1.8 Å resolution. FEBS Lett. **280:**379–382.